

## FLOOD VULNERABILITY AND RISK ASSESSMENT USING THE INTEGRATION OF ANALYTICAL HIERARCHY PROCESS (AHP), GIS, AND REMOTE SENSING: A CASE STUDY OF SOUTHERN OROMIA REGION

Dawit Girma Burayu<sup>1\*</sup>, Shankar Karuppannan<sup>2\*</sup>, Gemechu Shuniye<sup>1</sup>

<sup>1</sup>College Engineering and Technology, Wolkite University, Wolkite, Ethiopia

<sup>2</sup>Department of Applied Geology, School of Applied Natural Science, Adama Science and Technology University, Adama, Ethiopia

e-mail: <sup>1</sup> davegirma63@gmail.com <sup>2</sup> geoshankar1984@gmail.com

\*Corresponding Author

**Abstract:** In Ethiopia, southern Oromia is one of the regions affected by flooding, with the West Guji and Guji zones being the most frequently flooded places. People are exploiting natural vegetation for various purposes as a result of rapid population growth, resulting in deforestation and susceptibility to natural disasters such as floods. As a result, identifying flood-prone locations in great detail is essential for effective issue solving. Thus, this research was conducted to construct flood sensitive and flood risk mapping in southern Oromia utilizing the Remote Sensing, AHP (analytical hierarchy Process), and GIS. Eight flood-causing factors, such as drainage density, rainfall, elevation, slope, TWI, soil type, distance from the river, were developed in the GIS environment, and ERDAS Imagine software was employed to make land coverage and land usage data. The weighted overlay MCE approach was then used to construct a flood-sensitive map based on the AHP pairwise comparison of eigenvector value. To determine flood risk, population density, a vulnerable flood map, and land usage/land coverage layer were overlaid, having equal weightage. The flooding vulnerability outcome in the southern Oromia indicates that 0.3% (20.53km<sup>2</sup>), 31.4% (24986.4km<sup>2</sup>), 62 % (49310.6km<sup>2</sup>), 6.39% (5081.98km<sup>2</sup>), and 0.19% (148.866) is, very high, high, moderate, low, and very low flooding vulnerable region correspondingly. From the flood risk map, it was estimated that 2% (1587.3km<sup>2</sup>), 19.3% (15384.4km<sup>2</sup>), 75.5% (60071.7km<sup>2</sup>), and 3.15% (2505.3km<sup>2</sup>) of the area were endangered to very high, high, moderate, and low, flood risk levels correspondingly. As a result, the study will assist the relevant authorities in formulating development policies based on the existing flood danger and risk in the area.

**Keywords:** AHP, Flood, GIS, Remote sensing

### INTRODUCTION

Flooding is one of Ethiopia's utmost natural hazards, wreaking havoc on lives and businesses in various country zones (Gemechu Shale Ogato 2020). Flooding in Ethiopia is mostly caused by heavy rains and the terrain of the highlands and lowlands, which are linked by the main river basins' natural drainage system (Tasew 2022). Floods in the nation are most usually caused by lengthy periods of heavy rain, which leads rivers to overflow and inundate regions along riverbanks in the lowlands (Wondim 2016) (Assefa 2018) (Sitotaw Haile Erena 2019).

Floods are the most deadly, prevalent, and widespread catastrophic occurrence on the planet, among the natural phenomena capable of causing a calamity (Masoumi 2021) (Adhanom 2018). After droughts, floods are Africa's second and greatest environmental disaster (K. S. Vignesh 2020). The majority of nations in Sub-Saharan Africa face one or more natural risks. Floods wreak immense harm every year all around the world (Jonkman 2003). Floods may also have a considerable impact on public health, resulting in a decrease in socio-economic well-being. Floods killed roughly 93,000 people in the final 10 years of the 20th century, accounting for nearly 12% of all-natural catastrophe mortality (Jonkman 2003). As a result, flooding is a major topic of research, especially in developing nations like Africa and elsewhere. It is considered one of the greatest natural catastrophes, inflicting half of all infrastructure destruction worldwide. Floods have cost cities throughout the globe more than \$250 billion in damage, and flood intensity and frequency are growing. Recent floods have displaced 151,828 people in total (July and August 2020), with 100,176 individuals affected as of mid-August, including 40,731 individuals affected in Afar, 20,868 individuals affected in Somalia, and 40,731 individuals affected in Ethiopia, 1,125 individuals affected in Oromia (excluding the 141 individuals affected by a

DOI:

<https://opsearch.us/index.php/us/index>

landslide in East Wollega zone), 25,703 individuals affected in SNNP, and 11,749 individuals affected in Gambella (UNOCHA 2020).

Climate change forecasts show an increase in the incidence of severe rainfall events, both in terms of severity and frequency (Assefa 2018). Forecasted high-intensity rainfall events, when paired with changes in land-use patterns, may substantially modify the geographic range of future flood risk in a flood plain area, affecting the degree of river flooding and local flash floods (Baltas 2019). When a significant body of water overflows and submerges land, it is called a flood (Gemechu Shale Ogato 2020). Floods are one of nature's most devastating forces (Hunegnaw Desalegn 2020). Flood damages to farming lands and public utilities cost billions of dollars each year throughout the world, not to mention the loss of irreplaceable human and animal lives (Baltas 2019). A river exceeding its banks is the most common source of flooding (Legesse 2011). This might be caused by high rainfall mixed with insufficient canal capacity. An impediment in the riverbed may potentially cause over-spilling. When the main river reaches a high level, it may back up into the tributaries and adjacent lands, causing flooding at stream confluences.

Ethiopia is one of Sub-Saharan Africa's natural disaster-prone nations (drought, floods, etc.). Drought and flooding, along with poverty and rapid population increase, resulted in numerous individuals being victims of different calamities (Nigusse 2019). The huge rise in the number of individuals and locations impacted, as well as multiple fatalities, infrastructure, and property losses, indicate this. Flooding causes damage to both rural and urban regions. Direct damage to residential and non-residential structures is included in urban harm. The rural smash has harmed farm equipment, farmhouses, and infrastructure around agricultural areas (Hunegnaw Desalegn 2020). The farming injury was frequently lower than urban injury; as a result, farming injury assessments were lowered from time to time or just accounted for a small number of cases with simple methods and erratic estimations (Hunegnaw Desalegn 2020). Climate change's manifestations, such as erratic rainfall, frequent and severe floods, and droughts, have substantial effects on smallholder farming communities' livelihoods and security, making them increasingly susceptible in nations like Ethiopia. The unprecedented and exceptional volume of floods has alarmed several nations (Dereje Sufa Kenea 2020). The issues are more severe in both the river basin and urban regions (Nigusse 2019).

Inundation and bank erosion are the two most serious flood-related issues in Ethiopia. Furthermore, a sudden flood in the rural a few years ago wiped away buildings and infrastructure, killing many people and destroying agricultural land (ERCS 2010). The issue is influenced by the plain's topography, flow phenomena, and land cover (Hunegnaw Desalegn 2020). The main river and its tributaries overflowed, causing the river to flood. The majority of floods in the country occur as a result of rivers spreading out after prolonged rains, producing inundation of land along riverbanks on the flat plain (Dinka 2021).

Heavy rainfall and the topographies of the Highlands Mountain and lowlands plain, which have conventional drainage systems produced by the main river basins, are the primary causes of floods in Ethiopia, which inflict severe damage to human lives and livelihoods in sections of the nation (Adhanom 2018) (Hunegnaw Desalegn 2020) (Tasew 2022). Floods in the nation are most often caused by prolonged heavy rain, which causes rivers to overflow and inundates regions along riverbanks in the lowland plain (Assefa 2018) (Legesse 2011). The middle, upper, and downstream lowlands of the Awash River in Oromia and Afar; sections of Somalia's Wabe-Shebelle, Dawa Rivers, and Genale; and the low-lying Area of Gambella adjacent to Gilo, Baro, Alwero, and Akobo Rivers are among the key river flood-prone places; Flooding is also a threat in SNNPR's downstream regions adjacent to Bilate and Omo Rivers, as well as the huge floodplains near the Tana Lake and the riverbanks of the Megech, Gumera, and Rib Rivers in the Amhara area (ERCS 2010). Due to a lack of understanding regarding the causes of flood occurrences including overgrazing, afforestation, soil erosion, sand deposition, flood protection of the region, land degradation, and human settlement or site planning strategy, there was an information gap associated with floods in this particular region. Flooding and inadequate drainage are two significant environmental issues in the Oromia region's southern regions.

Although flooding cannot be completely avoided, its effects can be minimized with proper planning and management (Hunegnaw Desalegn 2020). Dams and non-structural measures (public awareness, legal instruments, forecasts, early alert systems, and rescue support) may help to lessen the impact of flood catastrophes on people and property (Gemechu Shale Ogato 2020). As a result,

flood protection measures are required for agricultural and other development operations in the region. As a result, flood vulnerability, risk mapping, and an awareness of society's current level of knowledge about flood disasters are required to lessen flood effects on economic and human settlements (Tasew 2022). GIS is one of the tools that may be utilized in flood level forecasting and management to help reduce human and economic losses by identifying regions that are at risk of flooding.

Geographic Information Systems (GIS) play an essential role in catastrophe analysis and management and have been employed in industrialized countries for the past two decades (Dinka 2021), (Dawit 2022), (Wondim 2016). Real-time flood and drought catastrophe monitoring, early warning systems, and quick damage assessment are all aided by GIS and advanced RS (remote sensing) techniques. A GIS is a technology that may help floodplain executives to identify regions in their communities that are prone to flooding (Adhanom 2018) (Sachchidanand Singh 2020). Geographic information is recorded in a database and may be searched and graphically presented using a GIS for analysis. Flood-prone locations may be recognized and targeted for mitigation or more severe floodplain management measures by overlapping or crossing different geographical layers. The primary benefit of utilizing GIS for flood investigations is that it provides a visual representation of floods and enables further analysis to assess flood damage (Assefa 2018). Flood vulnerability mapping determines the susceptibility degree of a particular location to floods (Gemechu Shale Ogato 2020). The procedure entails choosing biophysical and/or socio-economic variables about a location, then combining those elements with the decision maker's preferences to develop a composite appropriateness score (Kishore Chandra Swain 2020).

As a consequence of this process, a multi-parametric and multi-criteria decision-making dilemma arises. For acquiring geographical flood risk information, the geospatial strategy merging spatial analysis and remote sensing is particularly successful. Remote sensing aids in the collection, analysis, and different datasets integration for geographic decision-making, whereas spatial analysis aids in the collection, analysis, and integration of numerous datasets. To combine multi-criteria for assessing geographical vulnerability, spatial decision-making procedures must use weighting and ranking. The AHP is believed to be the most effective method for combining many criteria for particular decision-making to provide spatially sensitive data (Saaty 1980). In the AHP environment, multi-criteria layers are studied to produce a hierarchical structure that gives ranking and weighting with the help of users and experts (Sutapa Mukhopadhyay 2019). In the domains of flood control, including flood plain zoning, flood inundation mapping, and river morphological analyses, GIS and remote sensing techniques have proven to be effective.

Multiple experiments have been conducted to map vulnerability using geospatial methods utilizing diverse methodologies (Adhanom 2018) (Baltas 2019) (Dinka 2021) (Elijah Adesanya Adefisan 2015) (Muhammad Al-Amin Hoque 2019). Selecting appropriate criteria for each vulnerability element (for example, social and physical vulnerabilities and addressing potential) and their typical managing process improves the trustworthiness of vulnerability information. Other parameters, such as the scale of the study zone (regional/local), can affect the generation of comprehensive vulnerability data. Flood mitigation strategies benefit from detailed and precise vulnerable data (Wondim 2016) (Tasew 2022). However, because most current studies have been conducted using extremely narrow criteria and at a regional scale, a detailed flood vulnerability model is uncommon in the earlier documented reports. Another key challenge in vulnerability assessments is the selection of relevant components. Ethiopia is an extremely flood-prone region (Nigusse 2019). Several areas of the country are impacted each year. However, geospatial methods are rarely used in Ethiopian research to evaluate precise flood susceptibility. Few floods hazard, vulnerability, Risk, and management studies have been carried out, but most of them are concentrated in the northern part of Ethiopia, and without integrating all of the components of vulnerability, just a few criteria for measuring flood risk were examined. (Jiregna Nugusa Duressa 2021), (Hunegnaw Desalegn 2020), (Legesse 2011), (Adhanom 2018), (Assefa 2018), (Dereje Sufa Kenea 2020), and in the Middle, Upper, and Lower Awash sub-basin (Wondim 2016), (Dinka 2021), (Dereje Birhanu 2016), (Sitotaw Haile Erena 2019), (Dejene Tesema Bulti 2017). (Abirham Cherinet 2021) Flood risk, susceptibility, and risk have not yet been examined utilizing GIS and remote sensing techniques in the Southern Oromia area. As a result, this research will contribute to closing the knowledge gap and identifying flood-prone locations and vulnerable parts. The general goal of the

research was to use AHP, remote sensing, and GIS methods for estimating the flood susceptibility and risk in the Southern Oromia area. The research also looked at the elements that influence flood susceptibility and risk in this particular zone.

**MATERIALS AND METHODS**

The study was performed at Guji, West Guji, and Borena Zones, which are located in the Southern Oromia Region, Ethiopia. As illustrated in Figure 1, the Zones are positioned between 30 40' to 60 35' north latitudes and 360 30' to 400 0' east longitude. The zone's typical elevation ranges from 495m to 2936m above sea level, with a mean yearly precipitation of 1133.75mm. The Genale, Dawa, and Wabi Gastro River systems comprise the study zone. Before crossing the Ethio-Somali border, the Genale River is joined by the Dawa River to become the Genale–Dawa River, which drains the western part of the basin adjoining the Omo-gibe River basin (Dawit Girma and Belete Berhanu 2021). The Weyeb feeds the basin's north-eastern portion - the Gastro River, which joins the Genale–Dawa River at the Ethiopian-Somalia border to form the Jubbah River, which flows into the Indian Ocean (Ethiopian National Meteorological Agency, 2013).

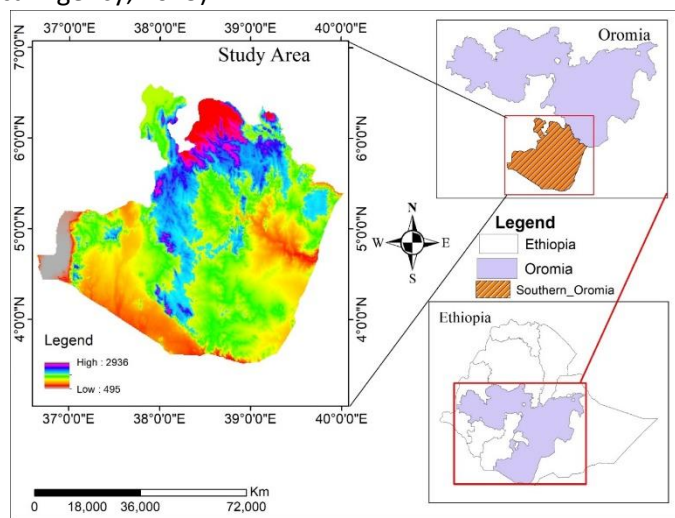


**Fig. 1** Study area map

The study was performed at Guji, West Guji, and Borena Zones, which are located in the Southern Oromia Region, Ethiopia. As illustrated in Figure 1, the Zones are positioned between 30 40' to 60 35' north latitudes and 360 30' to 400 0' east longitude. The zone's typical elevation ranges from 495m to 2936m above sea level, with a mean yearly precipitation of 1133.75mm. The Genale, Dawa, and Wabi Gastro River systems comprise the study zone. Before crossing the Ethio-Somali border, the Genale River is joined by the Dawa River to become the Genale–Dawa River, which drains the western part of the basin adjoining the Omo-gibe River basin (Dawit Girma and Belete Berhanu 2021). The Weyeb feeds the basin's north-eastern portion - the Gastro River, which joins the Genale–Dawa River at the Ethiopian-Somalia border to form the Jubbah River, which flows into the Indian Ocean (Ethiopian National Meteorological Agency, 2013).

The present study selected different criteria for flood vulnerability and risk assessment. Using geospatial techniques, to generate spatial criteria layers, we utilized a variety of data from diverse sources. This input comes from a variety of national and international sources. Table 1 details the sources and description of the dataset used in this study.

**Table 1** Data sources and description

No	Data Collected	Source of data	The function of the data
1	Annual Rainfall (1998-2016)	National Meteorological Agency (NMA)	To drive the Areal rainfall map by IDW
2	SRTM DEM 30	<a href="https://earthexplorer.usgs.gov/">https://earthexplorer.usgs.gov/</a>	To generate Elevation, drainage density, slope, TWI

3	Landsat 8 OLI/TIRS	<a href="https://landsatlook.usgs.gov/">https://landsatlook.usgs.gov/</a>	To generate LULC
4	Soil types	Ministry of Water, Irrigation, and Energy (MoWIE)	To drive soil thematic map
5	Census data	Ethiopian Statistical Agency	Population Density Map
6	River Network	Ministry of Water, Irrigation, and Energy (MoWIE)	Distance from River

The following steps are involved in creating a flood vulnerability map in this study: determining and characterizing the problem complexity, establishing the AHP model-based hierarchical framework for specified criteria, performing pair-wise comparison matrix analysis for preselected affecting parameters (binary comparison), assigning priorities values and determining relative weights for each parameter, measuring the consistency value for assessment and judgments, and preparing the flood vulnerability map. The AHP approach was utilized to determine the weighting of eight flood initiation variables that were responsible for determining the potential of individual components in causing flood susceptibility. For the calculation of relative weights, the impacting parameters were further divided into sub-categories based on their respective rankings.

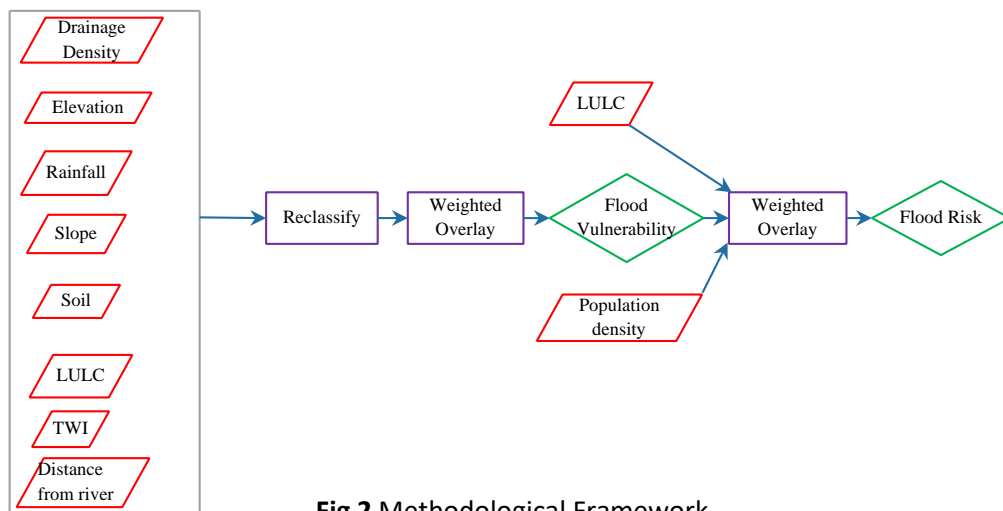


Fig 2 Methodological Framework

In this study, flood vulnerability and risk evaluation was done by characterizing Eight flood causing factors, such as drainage density, rainfall, elevation, slope, distance from the river, TWI and soil type, these were devised using ERDAS Imagine software in a GIS setting and land coverage/land use in a Remote Sensing environment. For constructing a crucial flood risk map, the chosen flood distribution characteristics were rasterized and classified in raster format, then weighted-overlaid using ArcGIS. The flood risk map, rasterized Land usage/land coverage, as well as population density map, was overlaid to develop a map of flood hazards.

Three significant parameters were examined when analyzing flooding risk in Southern Oromia: the population density, flooding vulnerability layer, and land cover/land usage type. In the weighted overlay method, these three criteria were given equal weight.

Because not all characteristics have the same impact on the distribution of flood risk, each parameter must be ranked (Dawit 2022). Each map was given a weighting and a pair-wise comparison matrix depending on the data (Saaty 1980). The rank/rate for categories in a layer and weights for individual component were allocated using the Multi-Criteria Decision Analysis approach based on AHP, and a pair-wise comparison matrix was constructed for individual map (Saaty 1980) (Dawit 2022) by considering Eight factors (drainage density, rainfall, elevation, slope, soil type, distance from the river, TWI, Population Density and land usage/coverage). Every condition is equated with other criteria on a

scale of 1 to 9, according to its significance, in square matrices (Table 2). The following procedures were used to compute the rank/rate for categories in a layer and the weights for thematic layers of individual component: The pairwise comparison matrix was carried out by using AHP techniques (Desalew Meseret Moges 2019) (Dawit 2022). The relative weight of their relevant classes was taken into account while calculating the cumulative weight of the primary criteria. Following that, using (Saaty 1980) AHP and weights normalized using the eigenvector technique, pairwise comparison matrices with provided weights to each thematic layers and sub-classes are generated. To assess the normalized weights of different thematic layers as well as their particular categories, the cr ratio (consistency) was determined according to (Saaty 1980). The following processes were used to calculate the CR of different thematic layers as well as their categories.

- 1)  $A = a_{ij}$  is a square matrix (Eq. 1) The lower triangular matrix was concluded by obtaining the reciprocal values of the top diagonal applying formula i.e.,  $a_{ij} = 1/a_{ji}$ , and the row I column j element was created.

$$A = \begin{bmatrix} \frac{P1}{P1} & \frac{P1}{Pj} & \frac{P1}{Pm} \\ \frac{Pi}{P1} & 1 & \frac{Pi}{Pm} \\ \frac{pn}{P1} & \frac{pn}{Pj} & \frac{pn}{Pn} \end{bmatrix} \quad (1)$$

- 2) Sum of all columns of the j matrix from (Eq. 1) in (Eq. 2)

$$\frac{p1}{p1} \dots \dots + \frac{Pi}{Pj} \dots \dots + \frac{Pn}{Pn} = \frac{\sum_{i=1}^n pi}{pi} \quad (2)$$

- 3) To generate normalized relative weights (Eq. 5), by dividing each component of the matrix i.e.,  $a_{ij} = pi/pj$  (Eq. 2) by (Eq.3)

$$\frac{\frac{Pi}{Pj}}{\frac{\sum_{i=1}^n Pi}{Pj}} = \frac{Pi}{Pj} * \frac{pj}{\sum_{i=1}^n Pi} = \frac{Pi}{\sum_{i=1}^n Pi} \quad (3)$$

- 4) The normalized primary Eigenvector (priority vector) is obtained by averaging over the rows (Eq. 6) to get the Rate (Ri) or I row weight (Wi). The total of all entries in the priority vector should be one since it is normalized.

$$\frac{Wi}{Ri} = \left[ \frac{Pi}{\sum_{i=1}^n Pi} \dots + \dots \frac{Pi}{\sum_{i=1}^n Pi} \right] * 1/n \quad (4)$$

Within each thematic layer, the consistency ratio was utilized to evaluate pair-wise comparison judgements (Saaty 1980). The percentage of reliability Scholars suggested that the process be repeated for matrices with a CR rating larger than 0.1 until the desired value of CR=0.1 is reached. CR value is calculated using (Eq. 5)

$$RC = \frac{Ci}{R} \quad (5)$$

Ratio index of Saaty is RI, while the Consistency index is CI. CI is a outcome of judgment consistency or consistency degree that is calculated by applying (Eq. 6).

$$CI = \frac{(\lambda_{max}-n)}{n-1} \quad (6)$$

where number of criteria is denoted by n, and Table 2 shows the RI value for n criteria.

**Table 2.** Saatty's, scale of intensity relative importance

Intensity of relative important	Definition
1	Equal importance
2	Weak or slight
3	Moderate importance
4	Moderate plus
5	Strong importance
6	Strong plus
7	Very strong
8	Very, very strong
9	Extremely importance

Source: (Saaty 1980)

To get  $k_{max}$ , multiply the normalized value by the appropriate weight (Eq. 6) and combine the product values to obtain  $k_{max}$  (Eq. 7)

$$\lambda_{max} = \sum_{i=1}^n W_i * \left( \frac{P_i}{\sum_{i=1}^n P_i} \right) \quad (7)$$

where  $k_{max}$  is the pair-wise comparison matrix's highest Eigenvalue. The alternative's priority is denoted by  $P_i$ , and the given rate/weight by  $W_i$ .

## RESULTS AND DISCUSSION

### Flood vulnerability factors analysis

The primary causes of flooding including rainfall, drainage density, elevation, slope, LULC, soil type, TWI, and distance from the river, have been considered for the vulnerability assessment inundation. Aside from earlier adjustments, the raster layers were categorized on the basis of their capacity to inundate the watershed.

### Rainfall Factor

Flooding is the most prevalent climate change-related catastrophic risk, according to many experts in the field of flood risk management, and floods have historically been the primary cause of death from natural disasters. The rainfall data from all rain gauge stations were generated using the IDW ("Inverse Distance Weighted") interpolation tool on the GIS platform and then transformed to a raster layer, which was then re-classed into five classes with an equal interval for the rainfall distribution map. The re-categorized precipitations were given a rating from one to five, with five suggesting substantial influence in resulting very high flood rate and one indicating extremely low effect insignificant extremely low flood rate. Class five areas have very heavy rainfall, whereas class one areas have extremely low rainfall. As a result, the greater rainfall value was classified as class 5 (>1212mm/year), the high placed as class 4 (978.624–1212.04mm/year), moderate listed as class 3 (826–9781mm/year), low listed to class 2 (700–826mm/year), and very low listed to class 1 (700mm/year).

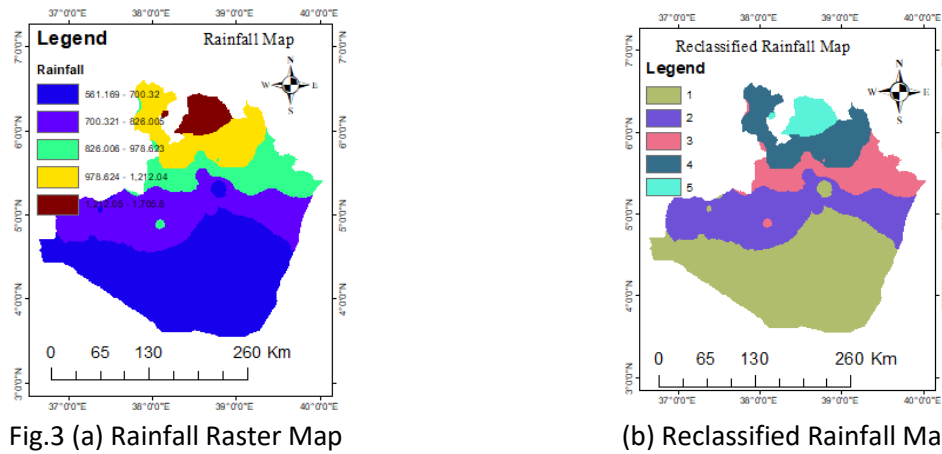


Fig.3 (a) Rainfall Raster Map

(b) Reclassified Rainfall Map

**Elevation factor**

The ArcGIS conversion tool was used to convert the DEM to elevation raster layers. The resulting TIN was used to generate the elevation raster layer. Using a normal classification technique, the elevation raster layers were re-classified into five sub-classes (Equal Interval). As a consequence, the classification method divided a wide range of feature values into small sub-ranges, enabling them to detect numeric intervals. The most recent number has been reclassified as a flood vulnerability rating. As a result, the flood significantly impacted the categorizing technique down to the smallest elevation. As a result, the flood has had a greater impact on class five upper elevations than on class one lower elevations. The flatter landscape was worth emphasizing at the lower level, whereas the steeper topography was worth mentioning at the higher elevation. It has been divided into five categories based on its flood risk. The lowest elevation region was severely intense, with floods ranking class five (<971m). Following that, high susceptibility is classified as class four (971.01–1297m), moderate vulnerability as class three (1297.01–1623.2m), and low vulnerability as class two (1623.3–2068.8m), and extremely low vulnerability as class one (>2069m).

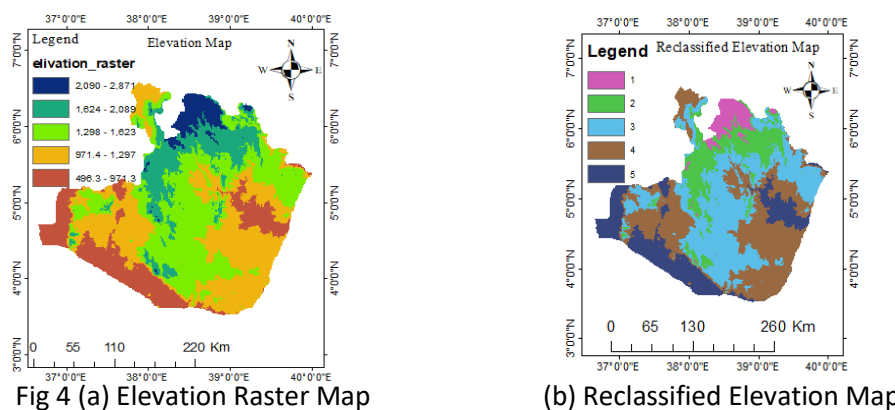


Fig 4 (a) Elevation Raster Map

(b) Reclassified Elevation Map

**Slope factor**

The slope of the study area was estimated by digitizing and altering a 20m contour interval characteristic rank from the Digital Elevation Model scale in a GIS environment. Using 3D Predictor Tools, the attributes were converted to a 3-D shapefile. Employing conversion tool into raster, the slope characteristic rank was transformed even further to raster. The raster layers of slope were then separated into five sub-groups using standard grouping procedures (equal intervals). The importance of the re-categorized slopes was graded on a scale of one to five, with five indicating a strong effect and a very high flood rate and one suggesting a very low influence and flood rate. As a consequence, a region having a very low slope was given a five, whereas a location with a very steep slope was given

a one. Such classification approach separates a wide range of feature values into uniformly sized sub-ranges, enabling the number of intervals to be set, whereas an Arc Map computes anyplace that does not. The flatter the terrain, the lower the slope value, and the steeper the topography, the greater the slope value. Slopes were classified into five categories on the basis of their proneness to floods. The regions with the shortest slopes are classified as class five (<2.393%) and are highly vulnerable to flooding. A high vulnerability was classified in class four (2.394–5.982%), a moderate vulnerability in class three (5.983–10.97%), and a low vulnerability in class two (10.98–17.96%), and a very low vulnerability in class one (>17.97%). The values were validated based on expert knowledge, local statistics, and the slope danger map's probable comprehensions, rather than breaking.

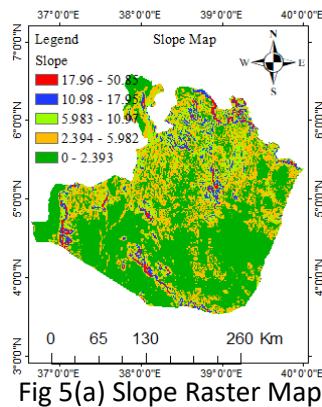
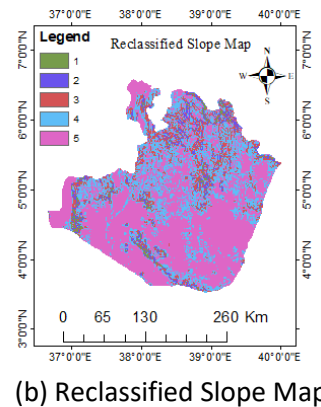


Fig 5(a) Slope Raster Map



(b) Reclassified Slope Map

**Drainage density factor**

It was estimated by dividing the drainage's overall length of all rivers and streams by the entire area of drainage. The research areas' drainage was obtained from digitized river systems in Southern Oromia and further rectified in a GIS framework, as shown in Figure 6. (a). The drainage density of the study region was also determined with spatial analyzer extension line density modules. The quantity per unit area is calculated by descending within a radius encircling each cell using the polyline characteristic. Using spatial analyzer extension, the drainage density of the Southern Oromia watershed was estimated. According to the classification technique illustrated in Figure 6(b), a region with a higher value is very heavily impacted by flood and is classified as class 5 (>0.095km/km<sup>2</sup>), high ranked as class 4 (0.0673–0.094km/km<sup>2</sup>), moderate ranked as class 3 (0.0432– 0.00672km/km<sup>2</sup>), low ranked as class 2 (0.0153–0.0431km/km<sup>2</sup>), and very low ranked as class 1 (<0.0152km/km<sup>2</sup>).

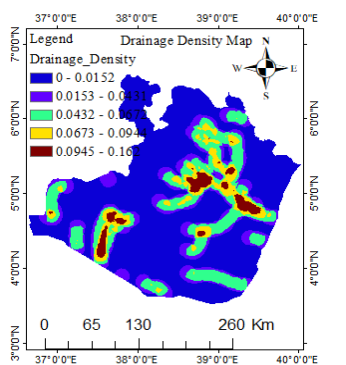
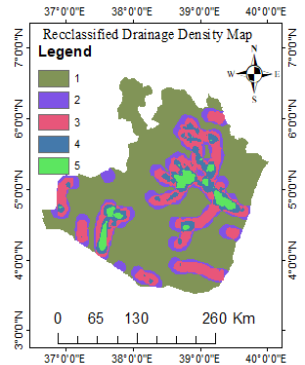


Fig 6 (a) Drainage Density Map



(b) Reclassified Drainage Density Map

**Land coverage/land usage factor**

The watershed area's land use/land cover was transferred to a classified land usage/land coverage form in five widely considered ranks and upgraded into a raster layer. Land use/land cover

types were also divided into five groups depending on their capacity to speed up or slow down inundation. As a result, cultivated land is rated as class 5, the bare area is listed as class 4, grassland is rated as a class 3, shrub and bushland are listed as class 2, and forest land has extremely low flood potential and is rated as class 1, as shown in Figures 11 and 12.

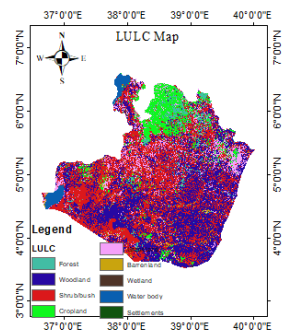
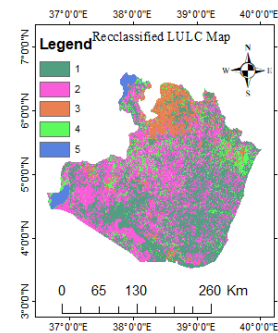


Fig 7 (a) LULC raster Map



(b) Reclassified LULC map

### Soil factor

There are several soil kinds; among them, five primary soil classifications are identified based on the Ethiopian Ministry of Water, Irrigation, and Energy's hydrologic soil-grouping method. The features of each soil type are explored based on the hydrologic soil grouping system. As a result, it was divided into five mutual clusters and rasterized. In addition, raster layer classes were reclassified into five categories, with a new value modification depending on their flood hazard rating. Sandy Loam is listed as class one, loamy sand is ranked as class two, Clay is ranked in class three, loam is ranked in class four, and Sandy clay is placed in class five because it has an extremely high potential to create an extremely high flood rate.

### TWI (Topographic wetness index)

TWI regulates water to flow overland by characterizing the geographical distribution of wetness. Flood mapping is heavily influenced by TWI. To measure how topography impacts runoff, flow direction, and flow accumulation, the TWI uses a physical index or indicator. Precision agriculture, customized rainfall-runoff modeling, and simulation of the geographical distribution of soil moisture are all applications of the index. The topographic profile regulates the distribution of water and the zones susceptible to water accumulation, according to a TWI. TWI and geomorphology, and the hydrographic position of a region, have a significant link. This indicator may anticipate saturated land surfaces with the potential to cause overland flow. TWI was computed in this study by examining the slope, flow accumulation, flow direction, and different geometric parameters using GIS software. The TWI computation produced a GIS data layer that shows regions with drainage depressions where water is expected to accumulate. Smaller TWI values suggest less possibility for ponding; higher TWI values signify that more upslope regions are drained and the local slope is moderate. The TWI layer was categorized into five categories, with the higher number indicating a greater TWI and the lower value indicating a lower TWI.

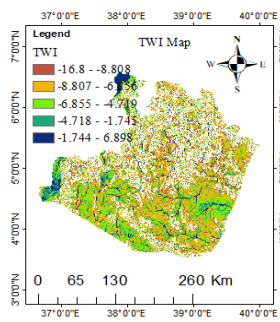
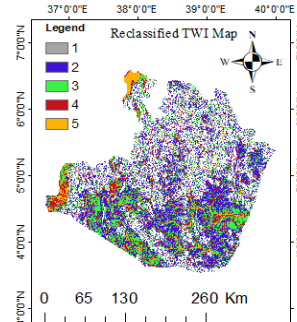


Fig 9 (a) TWI Map



(b) Reclassified TWI Map

**Population Density Factor**

The number of individuals per square kilometer in the Study area is calculated using the gross population density technique. Accordingly, population estimates for each village in the watershed were compared for 2016. The population shapefile was then converted into a raster layer using Conversion Tools/Feature to Raster. The equal interval technique was used to divide the data layer into five sub-factors, and additional values were assigned to boost the population density in flood-prone areas. The population density was classified based on the theory that a highly inhabited region is more prone to floods. Since of this, the most densely populated area is graded as a 5 as it is very vulnerable to floods. As a result of its lowest risk of flooding, the lowest population density group was given a rating of 1 on the scale.

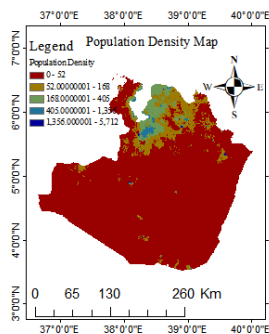
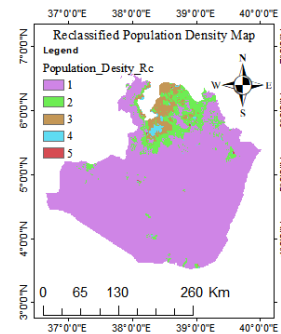


Fig 10 (a) Population Density Map



(b) Reclassified Population Density Map

**AHP spatial analysis Result**

The rasterized and categorized flood-causing components were weighted in the computation. The Analytic Hierarchy Process was utilized to create a pair-wise comparison for each map, and a 9-point significance scale was employed to arrange the pair-wise comparison. (Saaty 1980) Stated that AHP was a multi-criteria decision-making strategy that provided a rational method of evaluating and combining the consequences of several problems by linking various level-dependent, quantitative, and qualitative data. It was a technique for calculating the qualified relevance of a set of performances using pair-wise comparisons (Adhanom 2018) (Dawit 2022) (Hunegnaw Desalegn 2020). The relative importance of each component qualified to a separate factor was prioritized using weighting algorithms. In the weighted overlay, the higher the load, the more essential the element is in comparison to other variables. The consistency ratio was determined to be satisfactory at 0.1. To show a given paired weight, the computed consistency ratio of 0.084 was accepted. The slope is given high weight in the pairwise assessment, followed by elevation; land cover/land usage, drainage density, average precipitation, and soil group are also given substantial weights. Numerical algorithms describe the appropriateness of careful impact on the source of contribution needs, and how this influences each other through different mathematical or logical techniques of assessing disagreement. The

impact value range of 1 to 9 was given to each element using this method, and experts replicated the relationship result. Using the weighted linear combination approach, each map layer was stacked in a final GIS spatial evaluation for flood-sensitive zone imitation. An important phase in the AHP was the creation of a pair-wise comparison matrix, where each row indicates the qualified significance of one component to other. With a numerical scale ranging from 1 to 1/9, the relative significance of the two elements was estimated. The following was the correlation between a mathematical value and a lesser intensity: 1= equal importance, 1/3 = moderate, 1/5 = strong, 1/7 = very strong, 1/9 = extremely, on the other hand, high significant factors, were ranked between 1 and 9 (Dinka 2021), (Dawit 2022), (Gemechu Shale Ogato 2020), (K. S. Vignesh 2020), (Wondim 2016). The weighted linear combination approach was used to pile up each map layer in a final GIS spatial evaluation for flood risk zone imitation. The weighted linear combination system has now been superimposed, which was previously acceptable with any GIS scheme. With the weighted linear combination approach, a map of potentially flood-vulnerable southern Oromia may be generated that is almost exactly in its replication.

**Table 3.** Pair-wise comparison decimal matrixes

	SL	Elev.	RF	Soil	Dd.	LULC	Dist.	TWI
SL	1	3	3	3	5	5	7	7
Elev.	0.333	1	3	3	3	5	5	7
RF	0.333	0.333	1	3	3	3	5	5
Soil	0.333	0.333	0.333	1	3	3	3	5
Dd.	0.2	0.333	0.333	0.333	1	3	3	3
LULC	0.2	0.2	0.333	0.333	0.333	1	3	3
Dist.	0.143	0.2	0.2	0.333	0.333	0.333	1	3
TWI	0.143	0.143	0.2	0.2	0.333	0.333	0.333	1
SUM	2.685	5.542	8.399	11.199	15.999	20.666	27.333	34

**Table 4.** Normalized pairwise matrix calculated

	SL	Elev.	RF	Soil	Dd.	LULC	Dist.	TWI
SL	0.37	0.54	0.36	0.27	0.31	0.24	0.26	0.21
Elev.	0.12	0.18	0.36	0.27	0.19	0.24	0.18	0.21
RF	0.12	0.06	0.12	0.27	0.19	0.15	0.18	0.15
Soil	0.12	0.06	0.04	0.09	0.19	0.15	0.11	0.15
Dd.	0.07	0.06	0.04	0.03	0.06	0.15	0.11	0.09
LULC	0.07	0.04	0.04	0.03	0.02	0.05	0.11	0.09
Dist.	0.05	0.04	0.02	0.03	0.02	0.02	0.04	0.09
TWI	0.05	0.03	0.02	0.02	0.02	0.02	0.01	0.03

**Table 5.** Determined relative criterion weights

	SL	Elev.	RF	Soil	Dd.	LULC	Dist.	TWI	Weight	W (%)
SL	0.37	0.54	0.36	0.27	0.31	0.24	0.26	0.21	0.32	32
Elev.	0.12	0.18	0.36	0.27	0.19	0.24	0.18	0.21	0.22	22
RF	0.12	0.06	0.12	0.27	0.19	0.15	0.18	0.15	0.15	15
Soil	0.12	0.06	0.04	0.09	0.19	0.15	0.11	0.15	0.11	11
Dd.	0.07	0.06	0.04	0.03	0.06	0.15	0.11	0.09	0.08	8
LULC	0.07	0.04	0.04	0.03	0.02	0.05	0.11	0.09	0.06	6
Dist.	0.05	0.04	0.02	0.03	0.02	0.02	0.04	0.09	0.04	4

TWI	0.05	0.03	0.02	0.02	0.02	0.02	0.01	0.03	0.02	2
-----	------	------	------	------	------	------	------	------	------	---

Table 6 Weighted flood Vulnerability ranking

Flood Causative Criterion	Class	Vulnerability Class range	Vulnerability Class rating	Weightage (%)
Slope	0 - 2.39	Very Low	5	32
	2.39 - 5.98	Low	4	
	5.98 - 10.96	Moderate	3	
	10.965 - 17.94	High	2	
	17.94- 50.85	Very High	1	
Elevation	496.34 - 971.31	Very Low	5	22
	971.32 - 1,297.3	Low	4	
	1,297.4 - 1,623.2	Moderate	3	
	1,623.3 - 2,088.9	High	2	
	2,089 - 2,871.2	Very High	1	
Rainfall	561.16 - 700.32	Very Low	1	15
	700.32 - 826	Low	2	
	826- 978.62	Moderate	3	
	978.62- 1212.04	High	4	
	1212.04 - 1705.8	Very High	5	
LULC	Forest	Very Low	1	11
	Shrubs	Low	2	
	Croplands	Moderate	3	
	Bare land	High	4	
	Settlements	Very High	5	
Drainage Density	0 - 0.015	Very Low	1	8
	0.015 - 0.043	Low	2	
	0.043 - 0.067	Moderate	3	
	0.067- 0.094	High	4	
	0.094 - 0.16	Very High	5	
Soil Texture	Sandy Loam	Very Low	1	6
	Loamy Sand	Low	2	
	loam	Moderate	3	
	Sandy clay loam	High	4	
	Clay	Very High	5	
Distance from river	0 - 99.21	Very Low	5	4
	99.21 - 314.9	Low	4	
	314.9 - 509.02	Moderate	3	
	509.02 - 729.02	High	2	
	729.02 – 1100	Very High	1	
TWI	-16.8 - -8.808	Very Low	1	2
	-8.807 - -6.856	Low	2	
	-6.855 - -4.719	Moderate	3	
	-4.718 - -1.745	High	4	
	-1.744 - 6.898	Very High	5	

The computed Eigen Vector values have considered a coefficient of the specific flood factors that were utilized for land cover/land usage, elevation, slope, rainfall, drainage density, TWI, distance from river, and soil group layers to be combined within a weighted overlay in ArcGIS to generate the ultimate flood threats map of Southern Oromia by applying following equation introduced by (Saaty 1980).

$$FV = 0.32 * [Slope] + 0.22 * [elevation] + 0.15 * [Rainfall] + 0.11 * [Soil] + 0.08 * [drainage\ density] + 0.06 * [LULC] + 0.04 * [distance\ from\ river] + 0.02 * [TWI] \quad (8)$$

### Flood vulnerability map

The elevation, slope, rainfall, land cover/land usage, distance from the river, drainage density, soil types, and TWI were needed to construct a flood vulnerability map utilizing AHP and GIS or multi-criteria decision-making approaches. The flooding vulnerability outcome in the southern Oromia indicates that 0.19% (148.866), 6.39% (5081.98Km<sup>2</sup>), 62% (49310.6Km<sup>2</sup>), 31.4% (24986.4Km<sup>2</sup>), and 0.3% (20.53Km<sup>2</sup>) of the study area is, very low, low, moderate, high, and very high flooding vulnerable area respectively. It implies that more proportion of the Southern Oromia is a moderate and high flooding vulnerable zone. A flood risk analysis in Dire Dawa Town came to a similar result by (Dinka 2021) (Sitotaw Haile Erena 2019), Fetam watershed Upper Abbay Basin by (Hunegnaw Desalegn 2020), Fogera Woreda Northwest Ethiopia (Legesse 2011), Adama (Dejene Tesema Bulti 2017), Addis Ababa (Dereje Birhanu 2016), Bilate River basin (Tasew 2022) and lower Awash Basin (Wondim 2016).

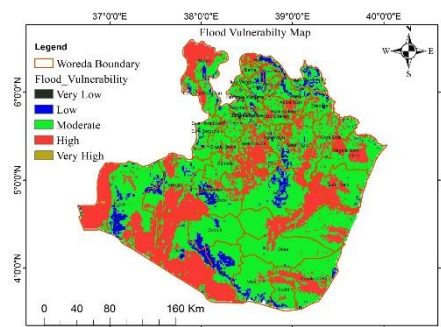


Fig 11 Flood Vulnerability Map

The investigation categorized Woredas in southern Oromia into various levels of flood risk to get additional information; Accordingly, Taltele woreda is under very high vulnerable, while Elwaya, Dilo, Melka Soda, Gumi Edalo, Arda Jila, Liben Negele town, Adola town, Gelana, Abaya, Odo shakiso, Dugda Dawa, Goro Dola, Dama, Saba Boru, Wadera, Miyo, Gomole, Ana Sora, Yaabelo, Moyale, are under High vulnerable class. Most Woreda in southern Oromia Like Dubluk, Dhas, Arero, Saro Barguda, Kercha, Wadera, Uruga, Haro Walabu, Girja, Adola, Bore, Bule Hora, Dire, Hambla Wamena, Birbisa Gojowa and Guchi are Moderately vulnerable to flood.

### Flood Risk Mapping

Flood risk mapping for Southern Oromia was done by combining the degree of flood vulnerability of the research region with population density and land use land cover factors at risk of flooding. It also demonstrated that 2% (1587.3 Km<sup>2</sup>), 19.3% (15384.4Km<sup>2</sup>), 75.5% (60071.7Km<sup>2</sup>), and 3.15% (2505.3Km<sup>2</sup>) of the study area were exposed to very high, high, moderate, and low, flood risk levels correspondingly. Our result reveals by (Adhanom 2018) (Abirham Cherinet 2021) (Assefa 2018) (Dereje Birhanu 2016) (Dinka 2021) (Gemechu Shale Ogato 2020) (Hunegnaw Desalegn 2020) (Tasew 2022) (Wondim 2016). Different degrees of danger are posed by the various risk factors investigated in this research. A very high flood risk region included the current Woredas in Southern Oromia,

including Taltele, Abaya, Bore, Melka Soda, Kercha, Gelana, and Negelle. Most Woredas Like Elwaya, Dilo, Melka Soda, Gumi Edalo, Arda Jila, Liben Negele town, Adola town, Gelana Abaya, Odo shakiso, Dugda Dawa, Goro Dola, Dama Saba Boru, Wadera, Miyo, Gomole, Ana Sora Yaabelo, Moyale, are under high and Dubluk, Dhas, Arero, Saro Barguda, Kercha, Wadera, Uruga, Haro Walabu, Girja, Adola, Bore, Bule Hora, Dire, Hambla Wamena, Birbisa Gojowa and Guchi are under moderate flood risk while few woredas in this study area are under low flood risk.

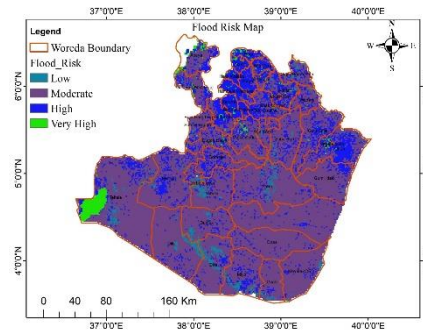


Fig 12 Flood Risk Map

## CONCLUSION

Flood-prone zones are often changing. As the country progresses, the type and extent of its vulnerability may alter. Flood vulnerability and risk mapping that is comprehensive requires precise information on field conditions, hydrologic data, and flood-defense structure elements. For Southern Oromia, this research used the analytical hierarchy process multi-criteria assessment technique approach based on expert choice and GIS-based analysis to develop a flood vulnerability zone map. This study examined eight flood causative elements based on the local context and flood susceptibility. Flood vulnerability and risk analysis may benefit from multi-criteria decision-making with the integration of AHP, which provides a step-by-step, flexible, and transparent method of evaluating based on end-user preferences, experts, knowledge, and decisions. Using the weighted overlay technique, a flood risk map of the region was created after allocating the determined weights. The flooding vulnerability outcomes in the southern Oromia indicate that 0.3% (20.53Km<sup>2</sup>), 31.4% (24986.4Km<sup>2</sup>), 62% (49310.6Km<sup>2</sup>), 6.39% (5081.98Km<sup>2</sup>), and 0.19% (148.866) of the study area is, very high, high, moderate, low, and very low flooding vulnerable area respectively. It implies that more proportion of the Southern Oromia is a moderate and high flooding vulnerable area. From the flood risk map, it was estimated that 2% (1587.3Km<sup>2</sup>), 19.3% (15384.4Km<sup>2</sup>), 75.5% (60071.7Km<sup>2</sup>), and 3.15% (2505.3Km<sup>2</sup>) of the study area were subjected to very high, high, moderate, and low, flood risk levels respectively. The study's risk factors demonstrate varying degrees of risk. The study's findings suggest that GIS-based multi-criteria analysis is an effective method for dealing with difficult challenges. As an alternate approach for flood inundation or demarcation of flood-prone areas, AHP may be utilized in conjunction with the GIS framework.

## REFERENCES

- Abirham Cherinet, Sadnur Worku. 2021. "Flood Inundation Mapping of Jigjiga-Town and Its Surrounding Environment: Using GIS & HEC-RAS Model ." *International Journal of Environmental Protection and Policy* 1-10.
- Adhanom, Amare Gebremedhin Nigusse and Okubay Gidey. 2018. "Flood Hazard and Flood Risk Vulnerability Mapping Using Geo-Spatial and MCDA around Adigrat, Tigray Region, Northern Ethiopia ." *Momona Ethiopian Journal of Science* 1-16.
- Assefa, Tesfay Hailekiros. 2018. "Flood Risk Assessment in Ethiopia." *Civil and Environmental Research* 1-6.

- Baltas, Elissavet Feloni Ioannis Mousadis and Evangelos. 2019. "Flood vulnerability assessment using a GIS-based multi-criteria approach—The case of Attica region." *Journal of Flood Risk Management published by Chartered Institution of Water and Environmental Management and John Wiley & Sons Ltd.* 2-15.
- Dawit Girma and Belete Berhanu. 2021. "Evaluation of the Performance of High-Resolution Satellite Based Rainfall Products for Stream Flow Simulation." *Journal of Civil & Environmental Engineering* 1-9.
- Dawit, Girma Burayu. 2022. "Identification of Groundwater Potential Zones Using AHP, GIS and RS Integration: A Case Study of Didessa Sub-Basin, Western Ethiopia." *Remote Sensing of Land* 1-15.
- Dejene Tesema Bulti, Boja Mekonnen, and Meseret Bekele Gelaye. 2017. "ASSESSMENT OF ADAMA CITY FLOOD RISK USING MULTICRITERIA APPROACH ." *Ethiopian Journal of Sciences and Sustainable Development* 1-18.
- Dereje Birhanu, Hyeonjun Kim, Cheolhee Jang and Sanghyun Park. 2016. "Flood Risk and Vulnerability of Addis Ababa City Due to Climate Change and Urbanization." *Elsevier* 1-5.
- Dereje Sufa Kenea, K P Deepdashan. 2020. "GIS Based Flood Hazard and Risk Assessment: A Case of Sibu Sire Woreda Oromia Region, Ethiopia." *Journal of Emerging Technologies and Innovative Research* 1-11.
- Dinka, Habtamu Tamiru and Megersa O. 2021. "Artificial Intelligence in Geospatial Analysis for Flood Vulnerability Assessment: A Case of Dire Dawa Watershed, Awash Basin, Ethiopia." *Hindawi the Scientific World Journal* 1-13.
- Elijah Adesanya Adefisan, Abdulkeem S. Bayo, Orimoloye Israel Ropo. 2015. "Application of Geo-Spatial Technology in Identifying Areas Vulnerable to Flooding in Ibadan Metropolis ." *Journal of Environment and Earth Science* 1-9.
- ERCS. 2010. "Floods Final report Emergency appeal no. MDRET003 GLIDE no. FL-2006-000112-ETH 4 March 2010. Period covered by this Final Report:." 6.
- Gemechu Shale Ogato, Amare Bantider, Ketema Abebe, and Davide Geneletti. 2020. "Geographic information system (GIS)-Based multicriteria analysis of flooding hazard and risk in Ambo Town and its watershed, West shoa zone, oromia regional State, Ethiopia." *Journal of Hydrology: Regional Studies* 1-15.
- H.T. Abdel Hamid, W. Wenlong and L. Qiaomin. 2020. "Environmental sensitivity of flash flood hazard using geospatial techniques ." *Global Journal of Environmental Science and Management* 1-14.
- Hunegnaw Desalegn, and Arega Mulu. 2020. "Flood vulnerability assessment using GIS at Fetam watershed, upper Abbay basin, Ethiopia." *Heliyon* 1-12.
- Jiregna Nugusa Duressa, Motuma Shiferaw Regasa. 2021. "Flood Inundation Mapping and Risk Analysis Case of Finchaa Lake ." *American Journal of Environmental Science and Engineering* 1-10.
- Jonkman, Ir. S.N. 2003. "Loss of life caused by floods: an overview of mortality statistics for worldwide floods ." *Delft Cluster-publication*.
- K. S. Vignesh, I. Anandakumar, Rajeev Ranjan, and Debashree Borah. 2020. "Flood vulnerability assessment using an integrated approach of multi-criteria decision-making model and geospatial techniques ." *Modeling Earth Systems and Environment*.
- Kishor Dandapat, Gopal Krishna Panda. 2017. "Flood vulnerability analysis and risk assessment using analytical hierarchy process." *Model. Earth Syst. Environ.* 2-18.
- Kishore Chandra Swain, Chiranjit Singha, and Laxmikanta Nayak. 2020. "Flood Susceptibility Mapping through the GIS-AHP Technique Using the Cloud." *International Journal of Geo-Information* 1-20.

- Legesse, Woubet Gashaw and Dagnachew. 2011. "Flood Hazard and Risk Assessment Using GIS and Remote Sensing in Fogera Woreda, Northwest Ethiopia." *Researchgate* 2-27.
- Masoumi, Zohreh. 2021. "Flood susceptibility assessment for ungauged sites in urban areas using spatial modeling." *Journal of Flood Risk Management published by Chartered Institution of Water and Environmental Management and John Wiley & Sons Ltd.* 1-15.
- Muhammad Al-Amin Hoque, Saima Tasfia, Naser Ahmed and Biswajeet Pradhan. 2019. "Assessing Spatial Flood Vulnerability at Kalapara Upazila in Bangladesh Using an Analytic Hierarchy Process." *MDPI Sensors* 1-17.
- Nigusse, Okubay Gidey Adhanom and Amare Gebremedhin. 2019. "Flood hazard and flood risk vulnerability mapping using geo-spatial and MCDA around Adigrat, Tigray Region, Northern Ethiopia ." *Ethiopian Journal of Science* 90-107.
- Saaty, T L. 1980. "The analytic hierarchy process." *McGraw-Hill, New York* 5.
- Sachchidanand Singh, Pankaj R. Dhote, Praveen K. Thakur, Arpit Chouksey and S. P. Aggarwal. 2020. "Identification of flash-floods-prone river reaches in Beas river basin using GIS-based multi-criteria technique: validation using field and satellite observations." *Natural Hazards* 1-23.
- Sitotaw Haile Erena, Hailu Worku and. 2019. "Urban flood vulnerability assessments: the case of Dire Dawa city, Ethiopia." *Natural Hazards* 2-23.
- Sutapa Mukhopadhyay, Subhankar Chakraborty and. 2019. "Assessing flood risk using analytical hierarchy process (AHP) and geographical information system (GIS): application in Coochbehar district of West Bengal, India." *Natural Hazards* 1-27.
- Tasew, eshale Tadesse Danbara Mulugeta Dadi Belete and Ayele Getachew. 2022. "Assessment of Flood Hazard Areas Using Remote Sensing and Spatial Information System in Bilate River Basin, Ethiopia." *Researchgate* 2-20.
- Wondim, Yirga Kebede. 2016. "Flood Hazard and Risk Assessment Using GIS and Remote Sensing in Lower Awash Sub-basin, Ethiopia ." *Journal of Environment and Earth Science* 1-18.

© 2023 by the authors. Submitted for possible open access publication under the terms and conditions of the Creative Commons Attribution (CC BY SA) license (<https://creativecommons.org/licenses/by-sa/4.0/>).

